IJEEC

International Journal of Electrical Engineering and Computing
Vol. 6, No. 2 (2022)

Original research paper
UDC 738.1:537.226/.228
DOI 10.7251/IJEEC2202048S

The Hazard of Electric Field Increment in the Damaged Silicon-Rubber and Porcelain Insulators

Asaad Shemshadi, Pourya Khorampour,

Department of Electrical Engineering, Arak University of Technology, Arak, Iran

E-mail address: p.a.shemshadi@gmail.com, poriyakhp@gmail.com

Abstract—**In power transmission lines, it is necessary to isolate the inherent voltage parts from each other and from zero potential. An insulator is defined as having a high degree of electrical insulation between the conductors and the brackets. Insulators also allow for mechanical conductivity of the conductor and ground. The presence of a broken insulator can alter the stress distribution. In this paper, the effect of mechanical insulation cracking (chattering) on electric field in two common types of insulators (porcelain and silicone rubber) and electric potential distribution models are analyzed. First, the electric field and electric potential patterns in the solid insulator are examined. In the following, the insulator is assumed to be broken, and the electric field and electric potential patterns for a broken insulator relative to the basic insulator shape are illustrated and compared. The results show that the presence of insulation cracking under dry and environmentally benign conditions affects the stress distribution pattern within and around the insulator. Finally, a comparison between the effect of fracture on the electric field and the potential distribution patterns in different parts of the insulator is discussed in detail.**

Keywords-component; Insulator Crack, Damaged Insulator Electrical Field, Porcelain, Silicon Rubber, FEM, HV.

I. INTRODUCTION

Compared to critical and expensive electrical network equipment, such as transformers and protection systems, isolators are cheap and cost-effective. However, these isolators play an important role in maintaining the most expensive equipment on the network. Furthermore, reliable transmission networks depend in part on transmission isolation [1,2]. On the one hand, these insulators must be prepared not only to withstand electrical stresses but also to withstand the mechanical forces that create the surrounding environment. Many factors can lead to the failure of isolation. Examples of internal and external insulation failure factors include radial cracks, pin corrosion, throwing of animal and human objects, and natural events [3, 4]. Insulators, especially porcelain, are likely to be damaged due to contraction and expansion at different temperatures. Furthermore, incorrect glazing on the insulating surface can also absorb moisture and dust. It should be noted that porcelain insulators can still serve the transmission line, even in damaged or near-damaged conditions. However, the length of time these insulators can last is unclear. This condition can cause variations in voltage distribution and electric field. Changes in voltage and electric field distribution can affect the insulation over its lifetime and ultimately cause the insulation to break after some time. In silicone rubber insulators conditions vary and, due to their high flexibility, the insulator is more rarely damaged. However, polymer insulators can break down, such as high electrical stress, natural events, rock throwing, projectiles, and so on [5,6]. Finite element methods are used to study the effect of fracture on electric fields and potential models [7, 8]. Therefore, the finite element method considers that the geometric complexity, the use of different types of constituents and the boundary conditions presents in the real problem, make it difficult to reach a definite solution. The use of an estimation solution that can be accepted in a limited time is inevitable and the finite element method is one of these options. The finite element method is a numerical method for obtaining approximate solutions for many problems in different fields. References [9,10] indicate contamination on the surface of the insulator by indicating contaminated water droplets that cause changes in the field and electrical potential of the insulator. These simulations are limited by the component methods. References [11,12] also analyze the field and the electric potential of two-dimensional polymeric insulators. The simulation was performed using the finite element method to break with the vulnerability point due to the field strength on these isolators. References [13,14] studied and distributed the field and electric potential on the surface of a polymeric insulator from the presence of contaminated spots under two-dimensional conditions using the MAXWELL software. In Reference [15,16], we calculate the field distribution and electric potential using the finite element method in a polymer insulator using a corona ring. References [16] also analyzed and inspected the corona ring on a 400 kV insulator. In this simulation, the design of the isolators and rigs was performed by the CATIA software and then transferred to the COMSOL software. It is important to note that CATIA software was used to draw the insulators and tower structure.

In this paper, the impact of fracture on the electric field and electric potential patterns for two common types of insulators (Porcelain and Silicon Rubber) will be analyzed and analyzed by COMSOL software. First, the electric field and the electric potential patterns on the healthy insulator will be examined. Then the insulator is broken and the electric field and electric potential patterns for the broken insulator corresponding to the healthy insulator are determined and compared. The results show that when there is a fracture at any location of the insulator, it affects the voltage distribution characteristics and the electric field. Finally, a comparison between the impact of fracture on the electric field and the potential distribution patterns on different portions of porcelain and silicon-rubber insulators will be made. It will be seen that the fracture increases the electric field around the insulator and also the fracture of the same potential lines closer together.

II. IMPLEMENTATION AND MODELING

Investigate the effect of lip stiffness on the potential splitting and modification of electric midget patterns on silicon insulators.

In order to start the studies on the insulators of electrical masts, according to the structure of Fig. 1, will design the mast and insulator in software with all details that regarded in Fig. 1, so simulate the 63kv rubber and Porcelain silicon insulator with the mast in CATIA software and transfer it to COMSOL software.

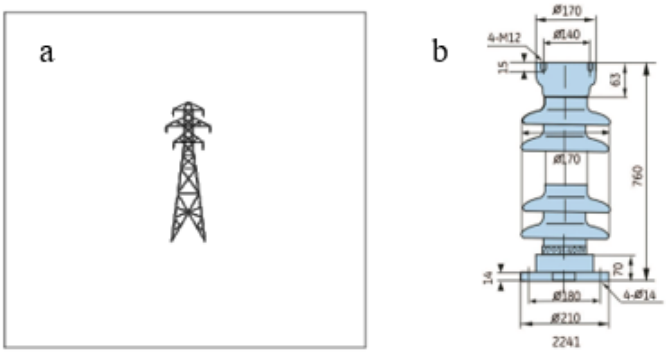

Figure 1. a: Outline of simulated space, b: Schematic of porcelain insulator

After designing the insulators and entering the details in the software and determining and defining the considered boundary conditions, we proceed to modeling and meshing in order to investigate and research the problem of breakage and destruction of the insulators. The mesh module is used in the software environment.

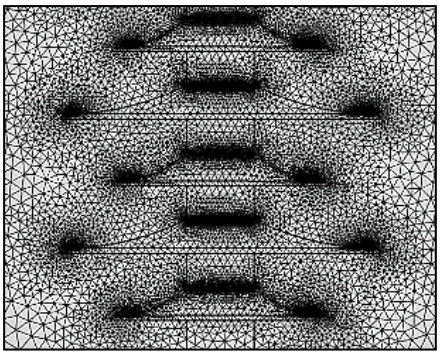

Figure 2. Silicon-rubber insulator meshing

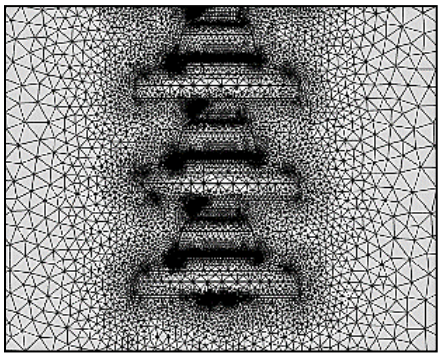

Figure 3. Porcelain insulator meshing

Actually, with Fig. 2 and 3 we start presents the application of the commercial software package COMSOL for the calculation of the electric field and potential distribution for a healthy insulator and for a mechanical fracture (broken) insulator. CATIA software is using for drawing only. Calculations, analyzes and conclusions were made for two types of insulators, silicon-rubber and porcelain insulators that are shown in Fig. 2 and 3 contain generated finite element meshes produced by COMSOL, therefore the meshing is illustrated in Fig. 2 and 3.

TABLE I. DEFINITION OF PARAMETER AND VARIABLE

FEM	Finite Element Method
HV	High Voltage
D	Electric flux density
σ	Electrical conductivity
ε_r	Relative permittivity of insulation
J_e	Current density
ρ	Electric charge density
$\emptyset$	Potential of nodes
F	Force matrix
K	Stiffness matrix
W	Weight function
Q	Electrical charge
R	Remaining vector

After finishing the mashing to solve the need for the desired formulas are as follows.

$$\nabla D = \rho_v \quad (1)$$

$$E = -\nabla V \quad (2)$$

To determine the intensity of the electric field, the combination of Maxwell's electromagnetic equations leads to the Poisson equation as shown below.

$$-\nabla[(\sigma + 2\pi f \varepsilon_0 \varepsilon_r)\nabla V - J_e] = 2\pi f \rho_0 \quad (3)$$

$$\nabla v = \frac{\partial^2 V}{\partial r^2} + \frac{1\partial V}{r\partial r} + \frac{\partial^2 V}{\partial Z^2} = -\frac{\rho}{\varepsilon_0 \varepsilon_r} \quad (4)$$

It should be noted that the electrical charges inside the insulator are negligible. Then $\sigma = J_e = \rho_0 = 0$

After specifying the physics, different parts of the software will apply the desired voltages.

To solve the problem presented in the paper and numerically solve the differential equations of the cable with spherical bubbles, we use the FEM, which provides a brief explanation of this method:

Finite Elements, the most important method of numerical solution of differential equations, will be formulated in Equations (5-7). This procedure generally involves the following three steps:

I. Divide the solution area of the differential equation by a finite number of components.

II. Find the solution of the differential equation at the points of the node created at the partition of the solution area and form the matrix apparatus needed to solve it.

III. Approximating the value of the differential equation function in each of the small components formed in step one by using the value of the function at three vertices.

$$D\frac{d^2\emptyset}{dx^2} + Q = 0 \qquad \emptyset_0 = \emptyset(0) \quad . \quad \emptyset_H = \emptyset(H) \quad (5)$$

$$-\int_0^H W(x)\left(D\frac{d^2\emptyset}{x^2} + Q\right)dx = R(x) \neq 0 \quad (6)$$

$\emptyset$: is a mathematical function we would like to obtain its value in every point of the domain. D and Q are constant

R(x): is the residual value and demonstrates the difference between estimated value of solving function and the exact value. Furthermore $\emptyset$_0 and $\emptyset$_H are the value of function in the boundaries 0 and H consequently.

Finite element method is divided into four sub-methods based on how to find the solution at nodal points:

a) Collocation Method, if W(x)=δ(x-xi)

b) Subdomain Method, if W(x)=1

c) Least Square Method, if W(x)=R(x)

d) Galerkin Method, if W(x)=NS , it is important to note that professional software's like COMSOL use only this procedure to arrange the equations and other procedures are put away over time.

After constructing and solving the equation (6), the following matrix equation is formed, and the resulting nodal values are obtained:

$$[K][\emptyset] = [F] \quad (7)$$

So, in the second part briefly describes the finite element method (FEM) used as a solver in the COMSOL software package. A mathematical model based on a system of differential equations, equations (3), (4) or (5), (6) is used. The special solution of these equations has been obtain based on the known boundary conditions (the structure of tower has fixed zero value potential; two three phase overhead lines domain have 63 kV rms value with 120 degrees lagging comparing together. Furthermore, the boundary value at surface of all type of insulators is selected as dielectric shielding state. All over surrounding boundaries are set to zero value potential). The numerical solution is a set of numerous values at specific points within the space of interest (meshing points). Based on equation (4), we can see that the written mathematical model is valid for axisymmetric systems.

III. IMPLEMENTATION AND MODELING

After specifying the physics of the different parts, applied voltages, meshing and formulas we will solve the problem.

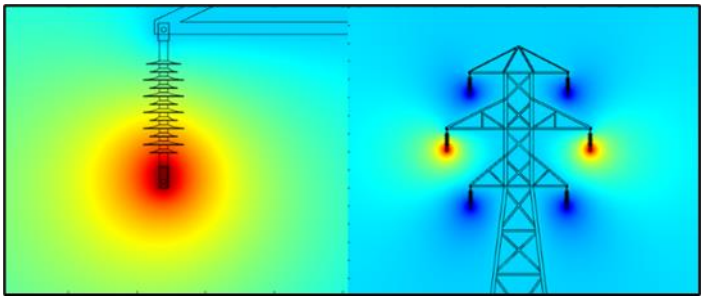

Figure 4. Electric potential pattern around silicon-rubber insulators

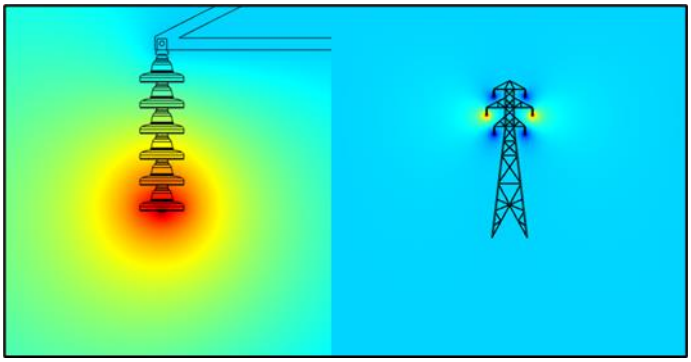

Figure 5. Electric potential pattern around porcelain insulators

Now indeed in the third chapter, Fig. 4 and 5 show the results of the calculation of the electric field for healthy insulators using the color spectrum. Fig. 6a and 6b show the results of the calculation of the electric field for broken insulators.

The electric field in the various parts of the simulated environment is shown in Fig. 4 and 5. It is clear from the pictures that there is a maximum field around the end of the insulator and will decrease as the field moves away.

For a better understanding as well as comparing the field in the broken insulator with the healthy insulator, all steps for the broken insulator will be repeated.

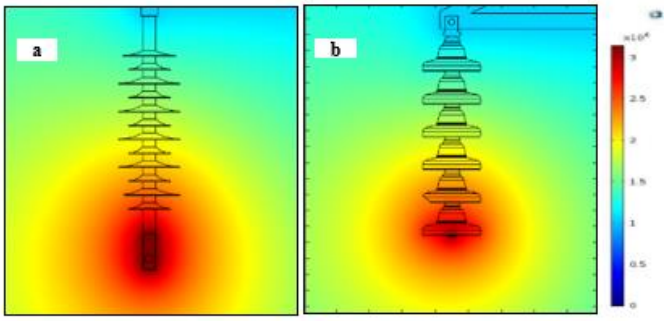

Figure 6. Calculation results of broken
a. silicon-rubber and b. porcelain insulators

The fracture occurred on the second plate from the bottom, where the field was broken in the sharp part created by the fracture and its corresponding point on the same plate in the insulator.

will now examine the impact of the fracture on different parts of silicon-rubber and porcelain insulators.

IV. SIMULATION AND DISCUSSION ON ELECTRICAL FIELD

Investigate the effect of lip stiffness on the potential splitting and modification of electric midget patterns on silicon insulators.

First, examine the effect of insulator bumps on the electric field.

A. Analysis of the second plate silicon-rubber insulator

first measure the electric field for the healthy insulator and then the broken insulator. From the bottom, break the second plate and compare it with the healthy one.

The part of the insulator to be broken is as shown below, and the diagram of the electric field value at the edge of the healthy insulator is 7501 V/m.

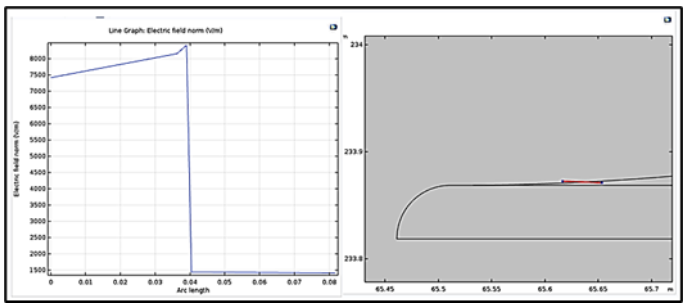

Figure 7. The electric field at the edge of the healthy insulator

After breaking the insulator at the point where the field is measured, the electric field at the breakpoint is increased to a significant 25351 V/m.

As the results show, with the occurrence of a fracture in the second plate silicon-rubber insulator, the electric field increases by 237.96%, which is very critical.

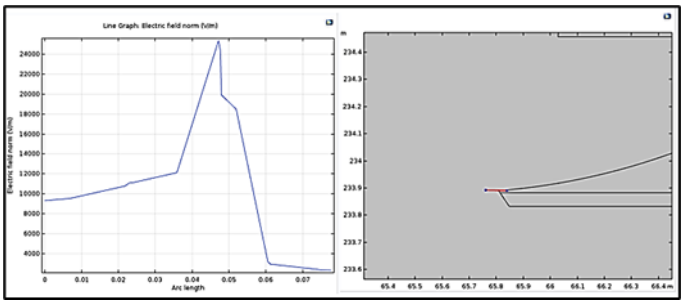

Figure 8. The electric field at the edge of the broken insulator

B. Analysis of the second plate porcelain insulator

According to the diagram, the electric field at the edge of the insulator is 8288 V/m.

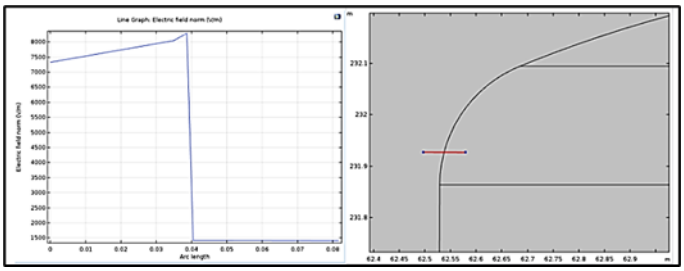

Figure 9. The electric field at the edge of the healthy insulator

After breaking the insulator, the electric field is broken at the sharp edge according to the 9818 V/m diagram, indicating an increase in the fracture field.

We see that with a fracture in the second plate porcelain insulator, the electric field increases by 18.46%, which is much less than in the second plate silicon-rubber insulator.

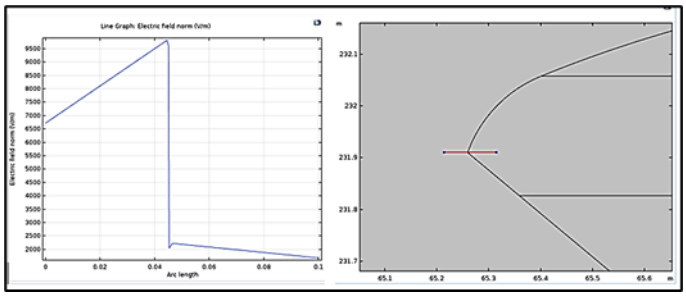

Figure 10. The electric field at the edge of the broken insulator

As expected, the fracture will produce sharp points that greatly increase the electric field.

Next, the impact of fracture on the electric field in the insulators above and below the fracture site will be investigated.

C. Analysis of the third plate silicon-rubber insulator

The electric field on the edge of a plate above the broken plate is 5502 V/m before breaking the insulator.

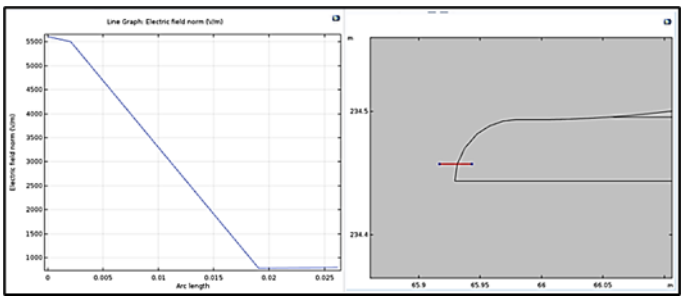

Figure 11. The electric field at the edge of the healthy insulator

After the second insulator plate is broken, the electric field in the specified area of the third plate increases to 5712V/m.

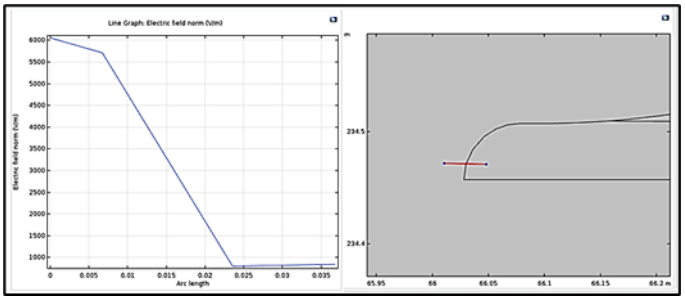

Figure 12. The electric field at the edge of the broken insulator

As the results show, with the occurrence of a fracture in the third plate silicon-rubber insulator, the electric field increases by 3.81%, that this is very small compared to the second plate silicon-rubber insulator.

D. Analysis of the third plate porcelain insulator

As shown in the Fig. 13, the edge of the third plate of the healthy insulator is 3571 V/m.

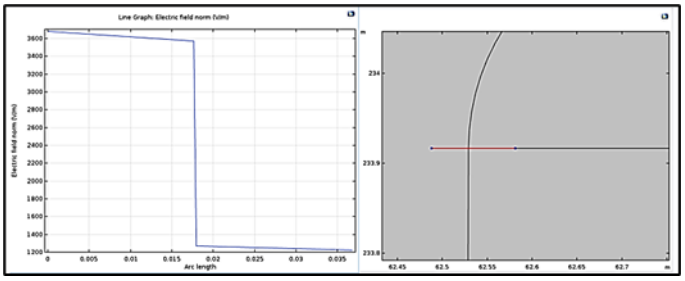

Figure 13. The electric field at the edge of the healthy insulator

The electric field in this part of the third plate of the insulator is broken according to the diagram of 3804 V/m, although slightly but increased, indicating that partial fracture of the insulator can affect other parts as well.

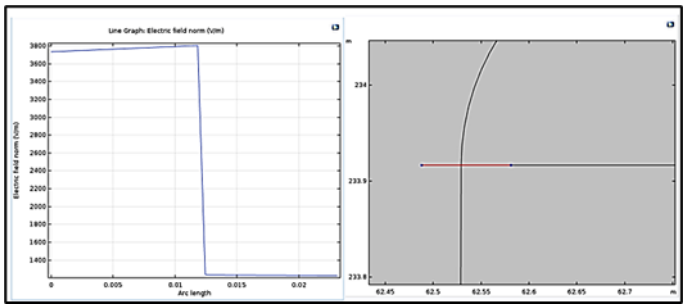

Figure 14. The electric field at the edge of the broken insulator

After examining the results, we find that the electric field in the third plate porcelain insulator increases by 6.52%, which is higher in the porcelain insulator than in the silicon-rubber insulator.

E. Analysis of the first plate silicon-rubber insulator

The diagram of the electric field on the marked part on the first plate of the healthy insulator is as follows, at the edge of the electric field insulator 8902 V/m.

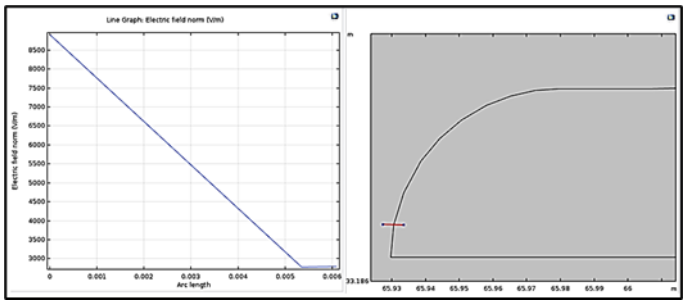

Figure 15. The electric field at the edge of the healthy insulator

The field at the edge examined for the broken edge insulator is 8955V/m.

Given the results, it is clear that with a fracture in the first plate silicon-rubber insulator, the electric field will increase by 0.59%, which is almost negligible.

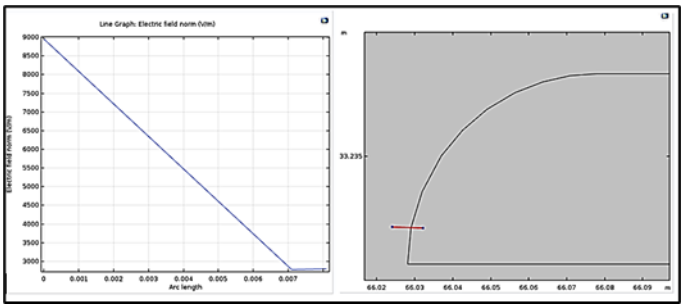

Figure 16. The electric field at the edge of the broken insulator

F. Analysis of the first plate porcelain insulator

In the healthy insulator, the field at the edge of the insulator is 13325V/m.

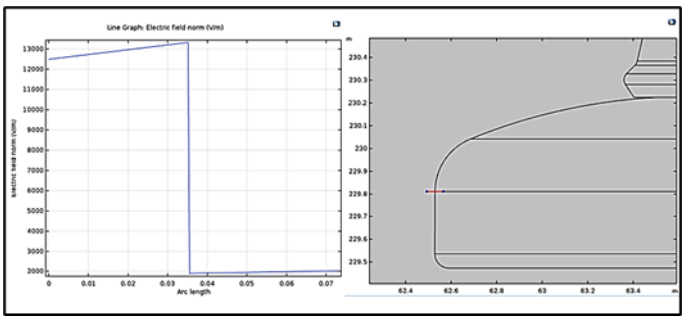

Figure 17. The electric field at the edge of the healthy insulator

The diagram of the electric field at the specified edge of the broken insulator is 13341V/m.

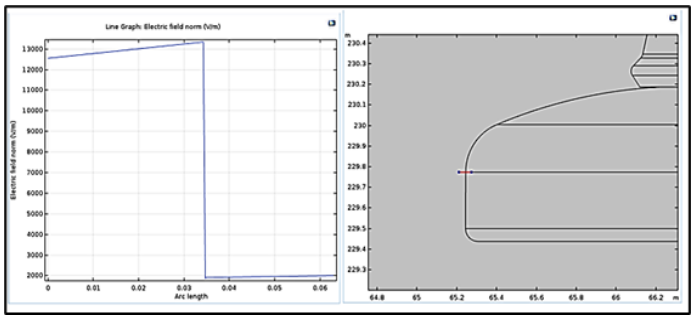

Figure 18. The electric field at the edge of the broken insulator

Examining the results, we see that the electric field increases by 0.12% in the third insulation, which is actually the case in porcelain insulation as in silicone insulation.

Based on the above analysis and the increase in the electric field at the fracture site and the points above and below the fracture site, it can be well approximated that the fracture at one point of the insulator affects the electric field of all the insulator points.

The results for porcelain insulators are similar to those of silicon rubber insulators, and these analyses show that no matter the insulator material, fractures increase the electric field in all insulators, which can lead to problems such as insulation and physical deformation of insulators. Leaving the insulator leads.

In Chapter 4 presents a detailed and useful analysis of the obtained data with the use of graphical representations.

At the end of the simulation results are summarized in the following table.

TABLE II. COMPARISON AND SUMMARY OF ELECTRIC FIELD INTENSITY IN HEALTHY AND FRACTURED INSULATORS

Case Study	*Third plate*	*Second plate*	*First plate*
Healthy porcelain insulator electric field (V/m)	3571	8288	13325
Electric field **of porcelain insulator broken** (V/m)	3804	9818	13341
Healthy silicon rubber insulator electric field (V/m)	5502	7501	8902
Electric field of silicon rubber insulator broken (V/m)	5712	25351	8955
Percentage of electric field increase in porcelain insulator broken (V/m)	0.6	15.5	0.1
Percentage of electric field increase in **silicon rubber** insulator broken (V/m)	3.6	70	0.6

Even if an insulator chain is composed of identical insulators, the potential distribution on the insulator chain is not uniform. At first glance, it may seem that the distribution of potential on this chain will be uniform. But because in each insulator between the upper and lower metal parts, between the metal parts with the body and the arm and the conductor of the capacitor transmission line, the existence of these capacitors causes an uneven distribution of potential across the insulator chain. Now, in the event of a bump or break in the insulator, this uneven distribution becomes much more severe and ultimately destroys the insulator.

In operation, the lower insulator (connected to the line conductor) has the highest potential difference and the high insulator (connected to the rig arm) has the lowest potential difference, so the occurrence of brittleness or failure on the upper insulators is less than your lower insulators.

In general, this happening reduces the useful efficiency of the insulator chain, which means that it reduces the amount of insulating property.

V. SIMULATION AND DISCUSSION ON ELECTRIC POTENTIAL

Then, examine the effect of insulator bumps on the electric potential.

A. The effect of fracture on the change of electrical potential patterns in silicon-rubber insulators

The potential energy of energy moving on a horizontal surface is neither decreased nor increased; such levels are called potential levels. The potential level is not a physical level but a mathematical description.

According to Equation (2) the electric potential increases in the opposite direction to the electric field, so it is expected that the electric potential will increase as a result of the insulator fracture, especially at the sharp point that results in a sharp increase in the field.

The simulation of the potential lines around the mast and porcelain insulator is illustrated below.

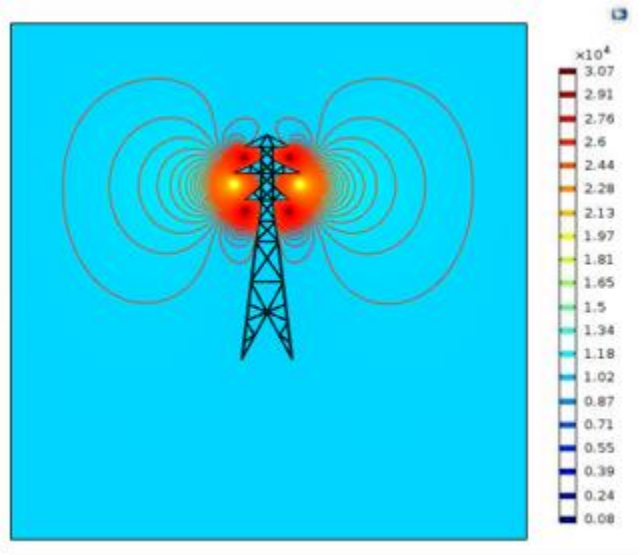

Figure 19. Potential lines around the tower and porcelain insulator

The potential lines in the figure are quite clear, since the difference of the electric field in the non-fractured parts of the two insulators is negligible, and the difference in the electric potential lines in the two forms is not very small and visible. Only the broken sharp point will be examined.

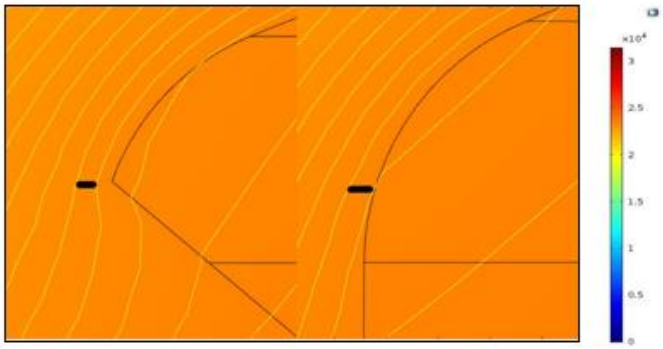

Figure 20. Lines of potential in healthy and broken porcelain insulators

B. The effect of fracture on the change of electrical potential patterns in porcelain insulators

The potential lines around the silicon rubber mats and insulator are outlined below.

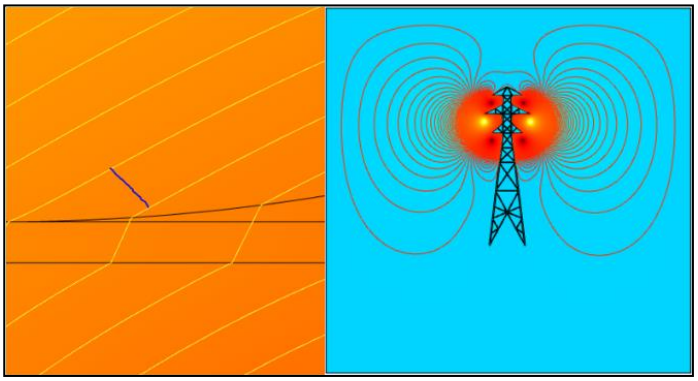

Figure 21. Electric potential patterns of healthy silicone-rubber insulators

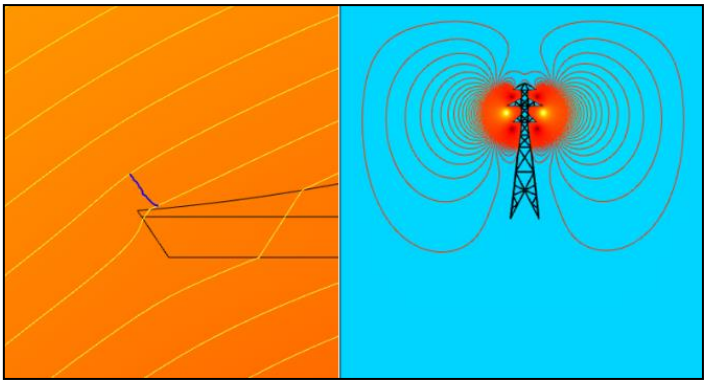

Figure 22. Electric potential patterns of broken silicone-rubber insulators

can see that fractures bring the electric potential lines closer together. So, as expected, the potential lines in the broken lip insulator, especially in the tip edges, are much closer together. Indeed Chapter 5 explains the effect of insulator bumps on the electric potential. Equipotential lines are drawn based on the calculated electric field distribution in the space of interest, which means that space includes both the "left" and "right" insulators.

VI. CONCLUSION

Investigate After simulating and analyzing the results, It is quite clear that at the fracture site, the nearer the bounds of the same potential, the greater the potential difference between the electrons and the potential changes, and as expected with the increase of the electric field, the electric potential has also increased.

Generally, by analyzing and identifying the potential increase and electric field at the fracture site as well as above and below the points, it can be said that fracture at one point of the insulator affects all the insulator points and the non-uniform changes of the potential and electric field distribution. Also, depending on the number of lip bumps or fractures, it may eliminate the insulator.

Finally, in general, the following analyzes are summarized as conclusions:

- The lips create sharp points where the electric field increases sharply.
- Fracture increases the electric field throughout the insulator, but it has more impact on the higher parts of the fracture.
- Fracture brings the potential of the lines closer together.
- Increasing the electric field is proportional to the potential of the lines getting closer.

In the end, a number of strategies to reduce the occurrence of insect fractures include the use of cover, modification of transport, maintenance of safer warehouses, utilization of skilled personnel when installing and using appropriate technologies such as nanotechnology in construction, Insulators for greater cohesion.

Appendix. Dimensions of insulator

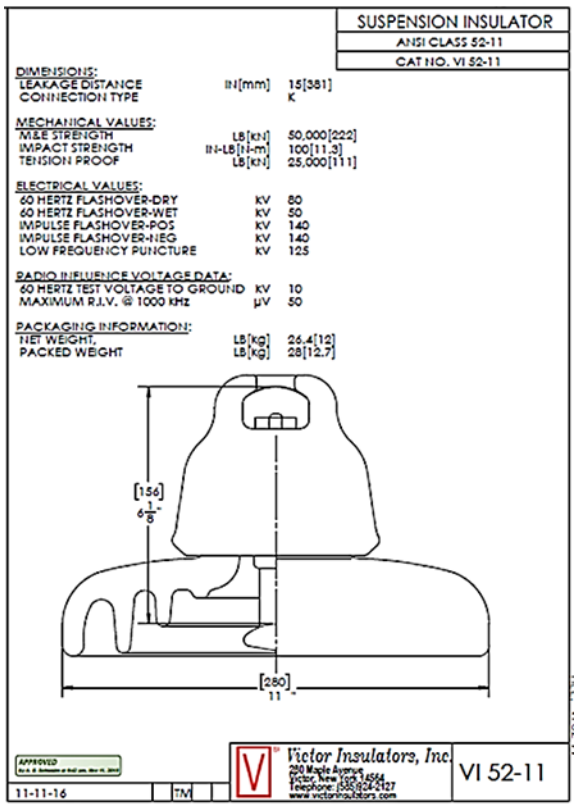

ACKNOWLEDGMENT

The authors declare no potential conflict of interest regarding the publication of this work. In addition, the ethical issues including plagiarism, informed consent, misconduct, data fabrication and, or falsification, double publication and, or submission, and redundancy have been completely witnessed by the authors.

REFERENCES

[1] J. Mackevich and M. Shah, "Polymer outdoor insulating materials. Part I: Comparison of porcelain and polymer electrical insulation," *IEEE Electrical Insulation Magazine*, vol. 13, no. 3, pp. 5-12, 1997.

[2] L. Ding, J. Wang, J. and Y. Mei, "Damaged Insulator Detection Based on Matching Network", 2nd International Conference on Power Electronics and Computer Applications (ICPECA), pp. 116-119, 2022.

[3] C. Spellman, H. Young, A. Haddad, A. Rowlands, and R. Waters, "Survey of polymeric insulator ageing factors," in *1999 Eleventh International Symposium on High Voltage Engineering*, vol. 4, pp. 160-163, 1999.

[4] J. Burnham and R. Waidelich, "Gunshot damage to ceramic and nonceramic insulators," *IEEE transactions on power delivery*, vol. 12, no. 4, pp. 1651-1656, 1997.

[5] S. Chandrasekar, C. Kalaivanan, A. Cavallini, and G. C. Montanari, "Investigations on leakage current and phase angle characteristics of porcelain and polymeric insulator under contaminated conditions," *IEEE Transactions on Dielectrics and Electrical Insulation*, vol. 16, no. 2, pp. 574-583, 2009.

[6] A. Okerinde, L. Shamir, W. Hsu and T. Theis, "Automatic detection of damaged electrical insulators in power-lines using deep learning", Thirty-fourth Conference on Neural Information Processing Systems (NeurIPS), 2020.

[7] R. Abd-Rahman, A. Haddad, N. Harid, and H. Griffiths, "Stress control on polymeric outdoor insulators using zinc oxide microvaristor composites," *IEEE Transactions on Dielectrics and Electrical Insulation*, vol. 19, no. 2, pp. 705-713, 2012.

[8] B. S. Reddy, N. Sultan, P. Monika, B. Pooja, O. Salma, and K. Ravishankar, "Simulation of potential and electric field for high voltage ceramic disc insulators," in *2010 5th International Conference on Industrial and Information Systems*, pp. 526-531,2010.

[9] P. M. Pakpahan, "Influences of Water Droplet Size and Contact Angle on the Electric Field and Potential Distributions on an Insulator surface," in *2006 IEEE 8th International Conference on Properties & applications of Dielectric Materials*, pp. 889-892, 2006.

[10] A. Okerinde, L. Shamir, W. Hsu and T. Theis, " Deep learning architecture that identifies damaged electrical insulators in power lines", arXiv preprint arXiv, 2021.

[11] B. S. Reddy, A. Kumar, A. Shashikala, and K. Ravishankar, "Electric Field Modelling of Composite High Voltage Insulators," in *2009 Annual IEEE India Conference*, 2009.

[12] A. A. Salem, K. Y. Lau, W. Rahiman, "Pollution Flashover Characteristics of Coated Insulators under Different Profiles of Coating Damage. Coatings", 11(10), p.1194, 2021.

[13] D. Jang, K. Lim, and M. Han, "Analysis of electric field distribution on the surface of polymer post insulator used in electric railway catenary system,", *International Conference on Condition Monitoring and Diagnosis*, 2008: IEEE, pp. 752-755, 2008.

[14] K. Mukhopadhyaya, "A Review on Insulators in Transmission Line Progress and Comparative Studies", ICT Analysis and Applications, pp.179-191, 2022.

[15] D. Stefanini, J. Seifert, M. Clemens, and D. Weida, "Three dimensional FEM electrical field calculations for EHV composite insulator strings," in *2010 IEEE International Power Modulator and High Voltage Conference*, pp. 238-242,2010.

[16] E. Al Murawwi and A. El-Hag, "Corona ring design for a 400 kV non-ceramic insulator", *2nd International Conference on Electric Power and Energy Conversion Systems (EPECS)*, 2011: IEEE, pp. 1-4. 2011.

Asaad Shemshadi was born on 1 November 1979. He received the B.Sc. degree from Shiraz University, in 2003, the M.Sc. degree from Kashan University, in 2007, and Ph.D. from Khaje Nasir Toosi University of Technology in 2014, Tehran, Iran, all in electrical engineering. Since 2016, he has worked as an assistant professor and a member of the academic staff of Arak University of Technology. His main research interests are vacuum interrupters design and analysis, high voltage simulations, DGA techniques, plasma modeling, high voltage equipment optimized design and transients in the vacuum arc quenching process.

Pourya Khorampour was born on 14 September 1996. He received the B.Sc. and M.Sc. degree from Arak University of Technology as 1st rank, all in electrical engineering. Since 2018. He has worked as an invited teacher in Arak University of Technology. He is an elite expert in Ministry of Energy of Iran. He received funding for a visit study course at a German university by DAAD.